

Baseline filtering and peak reconstruction for haloscope-like axion searches

Andrea GALLO ROSSO^{*1}, Jan CONRAD¹, and Junu JEONG¹

¹Physics Department and Oskar Klein Centre, Stockholm University, Stockholm, Sweden

March 7, 2025

Abstract

Axions are well-motivated dark matter particles. Many experiments are looking for their experimental evidence. For haloscopes, the problem reduces to the identification of a peak above a noisy baseline. Its modeling, however, may be problematic. State-of-the-art analysis rely on the Savitzky-Golay (SG) filtering, which is intrinsically affected by any possible over fluctuation, leading to biased results. In this paper we study the efficiency that different extensions of SG can provide in the peak reconstruction in a standard haloscope-like experiment. We show that, once the correlations among bins are taken into account, there is no appreciable difference. The standard SG remains the advisable choice because of its numerical efficiency.

1 Introduction

Strong evidences in astronomy and cosmology [1–7] suggest that about 85% of the matter in our universe does not belong to the Standard Model of particle physics. The question around its fundamental nature is one of the most important open problem in physics, with many candidates being proposed theoretically—see e.g. [8–11]. Among them, axions hold as one of the best motivated. They were proposed as pseudoscalar particles solving the strong CP problem [12–15], initially by Peccei and Quinn [16, 17], and then by Weinberg [18] and Wilczek [19]. A few years later, it was realized that axions have the right properties to explain dark matter [20–22]. Axions are spin-0, stable, massive particles. They interact weakly with the particles of the Standard Model, and can be produced (cold and with the right abundance) in the early Universe.

^{*}andrea.gallo.rosso@fysik.su.se.

The goal to detect axions in a laboratory is driving a titanic experimental effort [23–28], with the current goal set by the theoretical benchmarks of Kim-Shifman-Vainshtein-Zakharov (KSVZ) [29, 30] and Dine-Fischler-Srednicki-Zhitnitskii (DFSZ) [31, 32] models.

At present, the most promising technology to detect axions try to measure their coupling with photons. Resonant cavities, or haloscopes [33, 34] have proven themselves able to reach the sensitivity goal for masses below $\sim 1 \text{ eV}/c^2$ [35–38]. For such experiments, the sensitivity is enhanced by the resonant conversion of axions to photons, appearing as a narrow peak on top of the cavity profile (in the frequency domain). In many experiments, one of the main tasks that the analysis faces is to separate the possible signal from the known noise, in a problem of background subtraction [38–49].

In principle, the best possible approach would require a perfect knowledge of the background, which is in principle required by any likelihood approach (see e.g. [50]). In practice, this is not always possible. The most common procedure, based on [43], is to fit the the output of the DAQ pipeline (baseline) with a polynomial of a given degree, performed in a sliding window over the raw data. This is known as Savitzky-Golay (SG) filter [51]. Not only such an approach is free from background modeling, but it is also numerically efficient and its estimates are analytical and predictable. The latter are advantages that often outweigh the known issues, such as biases, numerical artifacts and underestimation of possible signals [52, 53].

In this paper, we will assess the underestimation that an axion-looking experiment may face, in the presence of a signal. We will make use of the definition [53] of peak reconstruction, as well as Monte Carlo estimation. We apply the calculation to the standard SG algorithm and to possible extension thought of as to circumvent the issue. Those methods are defined and discussed in Section 2. Section 3 presents the discussion about the quantification of the reconstructed efficiencies. Section 4 draws the conclusions.

2 Formalism and method

In the context of axion search, standard data are obtained by measuring the electromagnetic power coming out of a resonant cavity, in a setup similar e.g. to [54, 55]. In such a setup, the power coming from the cavity are initially collected in the frequency domain, discretized with a bandwidth resolution $\Delta\nu$. Typical values are $\Delta\nu \sim 100 \text{ Hz}$. On a large scale, in the absence of any axion signal, the thermal noise from a cavity follows a baseline $L(\nu_i) \equiv L_i = b_i$ which, ideally, is expected to be Lorentzian. However, the non-ideal nature of the amplification chain introduces in the component b_i features that are strongly dependent on the conditions of the apparatus and might be difficult to model.

On top of that, any axions depositing power in the cavity would appear

as an excess s_i distributed over many bins, following the profile of a boosted Maxwellian [56]. In the i -th bin corresponding to the frequency ν_i , the power signal s_i generated by the axion field can be written as:

$$s(\nu_i) = s_i = P_a \int_{\nu_a+i\Delta\nu}^{\nu_a+(i+1)\Delta\nu} f_a(\nu) d\nu \approx P_a \Delta\nu f_a(\nu_i), \quad (1)$$

where P_a is the total deposited power and $f_a(\nu)$ is normalized. Equation (1) applies when the bandwidth of the cavity is much greater than the axion linewidth.

The outcome of the experiment is constituted by the baseline L_i , which is composed by the component b_i , considered as a slow-varying background, and possibly by the signal s_i . That is, $L_i = b_i + s_i$. In turn, each collected bin $[\nu_i, \nu_i + \Delta\nu]$ represent a fluctuation of the noise power around the baseline, which is Gaussian with good approximation [43, 54]. This, assuming that the averaging process of the acquired spectra are sufficient.

In this paper, we focus on the extraction of the signal component s_i , when only the combination $L_i = b_i + s_i$ is known through the data $y(\nu_i) \equiv y_i$, and no description of b_i is available. This is usually the case for haloscopes and the first step in their analyses [43, 54]. In fact, they focus on the study of normalized fluctuations with respect to the baseline, which needs to be known. In other terms, we may consider

$$y_i \sim \text{Gaus}(L_i, \sigma), \quad (2)$$

where σ is the fluctuation of the power noise. The goal is to get a bin-to-bin estimate \hat{b}_i from the combination $L_i = b_i + s_i$ provided by the data y_i . Then, the estimated signal \hat{s}_i can be reconstructed as

$$\hat{s}_i = y_i - \hat{b}_i. \quad (3)$$

The standard procedure for the estimation of \hat{b}_i relies on the fact that b_i is smooth enough to be locally approximate as a polynomial, even on scales of hundreds of bins. Moreover, the scale of the variations is small with respect to the cavity profile. Then, one easy way to get \hat{b}_i would consist in clearing the data from any small-scale variations. In other word, “smoothing-out” L_i to get $\hat{b}_i \approx \hat{L}_i$.

The most common method to reach the goal is the SG filtering [51]. It is characterized by numerical efficiency, linearity and predictability of the results. In fact, SG filtering works by means of a polynomial fit of degree n on the N_p data points in the vicinity of the i -th bin. For instance, in the case of a symmetric window of half-length M around i , the windows becomes $\mathbf{x}_i = (i - M, i - M + 1, \dots, i, \dots, i + M)$, corresponding to a same number of measured values $\mathbf{y}_i = (y_{i-M}, y_{i-M+1}, \dots, y_i, \dots, y_{i+M})$. The output for the i -th data point corresponds to the fitting function $f_i(x)$ evaluated at

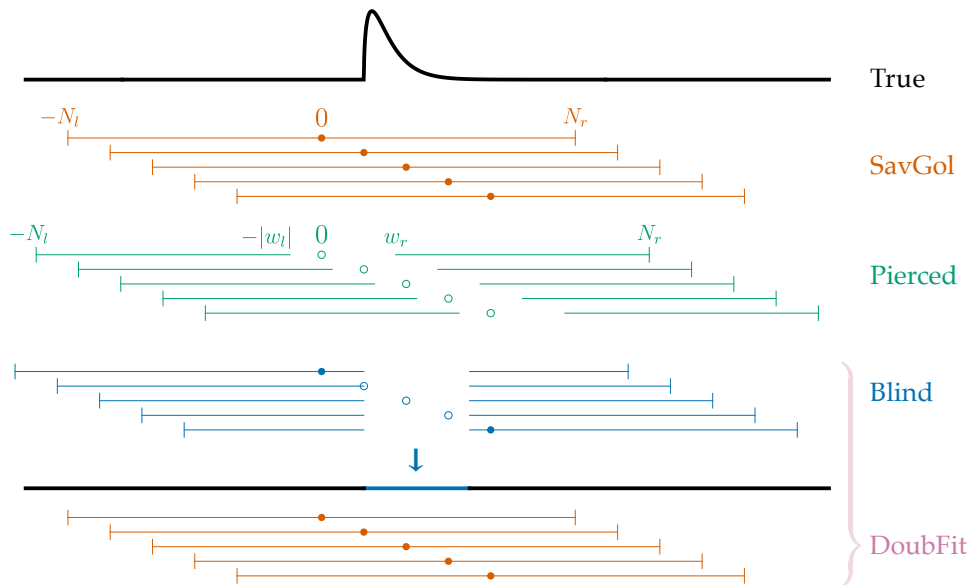


Figure 1: Graphical representation of the different filtering methods.

$x = i$. Because the problem is linear (see [57–59] and Appendix A) the output can be thought of as an averaged mean completely defined by a set of coefficients $\{c_k\}$:

$$f_i = \sum_{\{\ell\}} c_k y_{i+\ell} \equiv \hat{b}_i^{\text{SG}}. \quad (4)$$

2.1 Extension of SG filtering

Despite its numerical efficiency, SG filtering is intrinsically affected by the presence of any signal. This happens because the combination $L_i = b_i + s_i$ is used for an estimation for b_i only, which causes the results to be biased. As a consequence, the magnitude of s_i may get underestimated. This is shown graphically in Figure 2 (orange). There, the SG filter is applied to a peak rising from a flat baseline. Expressing the peak with respect to the filtered baseline return a result that is lower; i.e. the peak is shifted downwards.

This section presents possible extension of SG filtering aimed at overcoming this issue. After the methods are presented, they will be quantified in terms of their efficiency in recovering the signal. We will make use both of the standard definition of efficiency (see e.g. [53]) and a Monte Carlo-based analysis based on a full likelihood approach [60].

The first filtering algorithm will be denoted as ‘‘SavGol’’ and will correspond to a classic SG filtering over a symmetric window of length $N_p = N_l + N_r + 1$, where N_l (and N_r) are the number of points to the left (to the right) of the i -th filtered point. Therefore, this algorithm is fully defined by the values of the polynomial order n and the number of points N_p . With

respect to the former, the results presented in this paper are very mildly dependent on its exact value, provided that it is high enough ($n \gtrsim 2$). This is because of the smooth profile of the signal. In the following, we will set $n = 4$.

The number of points N_p needs to be sufficiently large to smooth out any possible signal peak from the baseline, but also small enough to preserve its features. In the following, it has been chosen to be 1201. This is a typical value for these kind of analysis on real data. The results remains very similar even for other values of N_p , provided they satisfy the conditions above. The problem of finding the optimal window length will be discussed in a following paper (in preparation).

The first extension of the standard SG filtering algorithm is aimed at getting rid of the biased data. We can achieve this goal by piercing the window around the i -th reconstructed point. In this way, the baseline for the bins belonging to the peak is reconstructed from data points that are away from the peak. In this case, the data that contribute to \hat{L}_i are such that $s_i \approx 0$. As a result, the reconstructed \hat{s}_i would be higher, and the bias would move to the tails. This scenario will be denoted as “Pierced.” In this case, the filtering window is defined by 4 parameters. In addition to N_l and N_r , two parameters define the hole around the filtered point, made up by $w_l > 0$ ignored points on the left-hand side and $w_r > 0$ ignored point on the right-hand side. That is,

$$k \in [-N_l, -w_l] \cup [w_r, N_r] \quad (5)$$

We optimized those parameters to get the best signal-to-noise ratio, while maintaining the number of total points to be equal to the “SavGol” case.

The third procedure avoids the bias by introducing a blinded region around the peak altogether. By construction, this filtering method allows for a perfect peak reconstruction (Figure 1 and 2, blue). This means to disregard all the bins within a certain window $k \in [0, k_{\text{sig}})$, large enough to cover the most of the signal—we recall that, because of (6), $i = 0$ marks precisely the start of the signal window.

This method will be denoted as “Blind.” It is dependent on the analyzed frequency, in that a different window is required for any positions of the peak, built in such a manner to exclude the peak region. In a real analysis, this means to run the filtering algorithm for each tested hypothesis. In other words, sliding a *set* of windows for each tested hypothesis, rather than sliding a single window for every hypothesis. Numerically, the task is largely facilitated by the construction of look-up tables. From the point of view of the code, the case is similar to the “Pierced” one, but with the four parameters w_l and w_r left free to assume negative values. This makes sense, if we want the hole to be between $-N_l$ and 0 or 0 and N_r —see (5). In the following, we will assume a blinded region of $N_{bl} = 250$ bins, while the filtering window is symmetrical with total length $N_p + N_{bl} = 1451$.

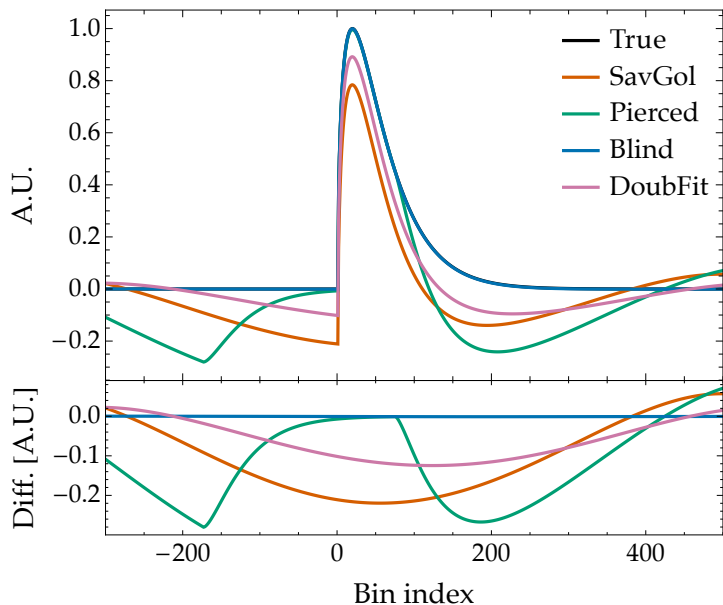


Figure 2: Reconstructed signal \hat{s}_i (3) from the (un-fluctuated) baseline $b_i + s_i$, where $b_i \equiv 0$ and s_i parameterized by equation (6). The right panel gives a graphical representation of the different filtering methods.

However, the amount of peak reduction in itself is not a good indication of the efficiency of the method. Up to this point we have focused just on the shape of the signal, disregarding any fluctuations and/or their correlations. As we will discuss in the next section, one should also consider the enhancement or suppression of the scale of the fluctuations which can further reduce or highlight any possible signal.

As we will show below, the standard SG filtering is characterized by the highest fluctuation suppression. For this reason, we introduce the last method, which aims to combine the unbiased results of the “Blind” method and the minimum correlation given by the “SavGol” one. In this procedure, denoted as “Double Fit” (or “DoubFit”), the “Blind” procedure is used to get the filtered point just in the blinded window. Then, a standard SG filtering is performed, with the data in the signal region replaced by the output of the “Blind” procedure.

3 Peak efficiency reconstruction

The scope of this paper is not the reconstruction of actual physical quantities but rather the comparison of different algorithm. Therefore, in order to quantify the problem, we follow the approach by [53].

Specifically, we will tackle the problem of the reconstruction of a peak

A	N_l	w_l	w_r	N_r	ξ'	ξ	$\delta_{\text{out}}/\delta_{\text{in}}$	ε_{SNR}
True	—	—	—	—	0.999 ± 0.045	1.001 ± 0.002	1.000	0.999 ± 0.002
SavGol	600	—	—	600	0.999 ± 0.045	0.817 ± 0.001	0.677	0.829 ± 0.001
Pierced	675	75	175	775	1.000 ± 0.045	1.161 ± 0.002	0.947	0.816 ± 0.001
Blind	725	—	—	775	0.999 ± 0.045	1.240 ± 0.002	0.999	0.806 ± 0.001
DoubFit	600	—	—	600	0.999 ± 0.045	1.006 ± 0.002	0.827	0.822 ± 0.001

Table 1: Parameters ξ' , ξ , $\delta_{\text{out}}/\delta_{\text{in}}$, and ε_{SNR} computed for the filtering methods discussed in Section 2.1.

above a flat baseline. In other words, without the features of the cavity profile. that is, $b_i \equiv 0$. Moreover, we will focus on the signal s_i as reproduced by the following toy parameterization, similar in shape to the boosted Maxwellian expected for axions:

$$s_i = \begin{cases} \delta_a e^{-0.03i} \sinh(\sqrt{0.03i}) & \text{for } i \geq 0; \\ 0 & \text{for } i < 0; \end{cases} \quad (6)$$

where δ_a is a normalization constant chosen according to our purposes. Because of its pure mathematical nature, we can simplify the problem even further by considering unitary variance for the fluctuated data, i.e. $y_i \sim \mathcal{N}(s_i, 1)$.

The efficiency in the peak reconstruction, ε_{SNR} , can be estimated by comparing the signal to noise ratios in input and output. Following definition of Ref. [53] (to which we address the reader for details) we consider:

$$\varepsilon_{\text{SNR}} = \frac{1}{\xi} \frac{\text{SNR}_{\text{out}}}{\text{SNR}_{\text{in}}} \simeq \frac{1}{\xi} \frac{\delta_{\text{out}}}{\delta_{\text{in}}}. \quad (7)$$

The ratio $\delta_{\text{out}}/\delta_{\text{in}}$ can be thought as an averaged sum of the estimated signal (3) over the unfiltered signal s_k over some window $k \in [0, k_{\text{sig}}]$:

$$\frac{\delta_{\text{out}}}{\delta_{\text{in}}} = \frac{\sum_{k=0}^{k_{\text{sig}}-1} s_k \hat{s}_k}{\sum_{k=0}^{k_{\text{sig}}-1} s_k^2}. \quad (8)$$

Here, s_k is given by (6) and \hat{s}_k by (3), with $b_k \equiv 0$. In our case, we will consider $k_{\text{sig}} = 250$, while the parameters of the different filtering methods can be found in Table 1.

The factor ξ , on the other hand, is a normalizing factor that compensates for the change in the scale of the fluctuations. Those arise from the bin-to-bin correlations caused by the filtering methods. The factor ξ can be thought as the standard deviation of \hat{s}_k^{add} , a weighted sum of \hat{s}_k within the signal window. That is:

$$\hat{s}_k^{\text{add}} = \frac{\sum_{k=0}^{k_{\text{sig}}-1} s_k \hat{s}'_k}{\sqrt{\sum_{k=0}^{k_{\text{sig}}-1} s_k^2}}. \quad (9)$$

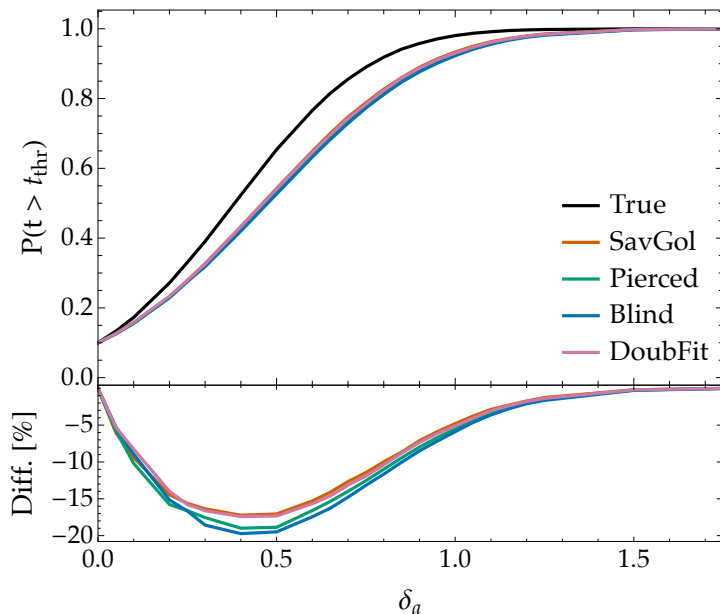


Figure 3: Top: probability of the claim of a discovery, as a function of δ_a , for different filtering methods, with $CL = 90\%$. Bottom: deviation of the different filtering methods with respect to the perfect baseline reconstruction (Monte Carlo truth, represented by the black solid line in the top plot).

In this case, however, \hat{s}'_k is built from the fluctuations of y_k when $s_k = 0$; i.e., $y_i \sim \mathcal{N}(b_i, 1) = \mathcal{N}(0, 1)$. That is, in our notation:

$$\hat{s}'_k = (y_k - \hat{b}_k)/\xi'. \quad (10)$$

Once again, ξ' preserves the magnitude of the standard deviation from y_k to \hat{s}'_k in the signal window. The value of the estimated parameters are reported in Table 1, for the different filtering methods presented in Section 2.1. In our case, we estimated ξ' , ξ by means of Monte Carlo evaluation on 2×10^5 samples.

Despite the SG filtering being the worse at recovering the height of the peak, the proposed alternatives get penalized by the correlations among bins, canceling out any potential gain.

3.1 Monte Carlo approach to the signal recovery

We can test the robustness of these conclusion by means of a simulated experiment. That is, a Monte Carlo-based likelihood approach built on the formalism presented in Ref. [60].

In this setting, we assume a value for the coupling δ_a . Then, pseudo-random data $y_i \sim \mathcal{N}(s_i, 1)$ are generated. They are then fed into the filtering algorithm in order to recover the reconstructed baseline. The noise

fluctuations are quantified according to their deviation with respect to the reconstructed baseline. This is similar to what would happen in a real analysis. Then, the test statistics t is computed,

$$t = \frac{\sum_i s_i y_i}{\sqrt{\sum_i s_i^2}}. \quad (11)$$

The value of t is compared against a threshold, t_{thr} , defined with respect to the null hypothesis ($\delta_a = 0$):¹

$$P(t > t_{\text{thr}} | \delta_a = 0) = 1 - CL, \quad (12)$$

where CL is the confidence level, which we assumed to be 90%. If $t > t_{\text{thr}}$, we claim that the null hypothesis has been rejected and that our set of data allows for the claim of a “discovery”.

We repeat the procedure for different values of δ_a , for different filtering algorithms, registering the fraction of successful experiments. This becomes our definition of efficiency. Note that t_{thr} is built from simulated data, too. Thus it automatically accounts for the correlations among bins, induced by the filtering procedures.

The values of $P(t > t_{\text{thr}})$ are shown in Figure 3 for the different filtering methods. By construction, all the methods converge at $1 - CL = 0.1$ for $\delta_a = 0$. For coupling δ_a strong enough, the signal becomes so strong that the null hypothesis is rejected with probability 1, regardless of the method used to recover the baseline. In between, we see that the performance of the filtering methods are all within a few percent, and under-perform with respect to the Monte Carlo truth (perfect knowledge of the baseline) up to 20%, in line with the outcome of Table 1.

The results are robust. In fact, the conclusions are the same if we apply the filtering methods to a baseline more similar to a real one (Figure 5, right). In this case, we attempted a reproduction of the standard aimed at a mature stage of the ALPHA experiment [61]. The baseline is assumed to have a functional form as described by [35], with cryogenic quality factor $Q \sim 10^5$ and a resonance of 10 GHz.

4 Conclusions

In conclusion, in this paper we have applied different extensions to the SG filtering to the problem of the reconstruction of a signal s_i , expressed as a peak over a slow-varying background b_i , when only the combination $L_i = b_i + s_i$ is known, and no description of b_i is available. We have applied the SG filtering, as well as possible extensions, to compensate for biased

¹Note that, in most axion analyses, the null hypothesis is defined as the existence of an axion.

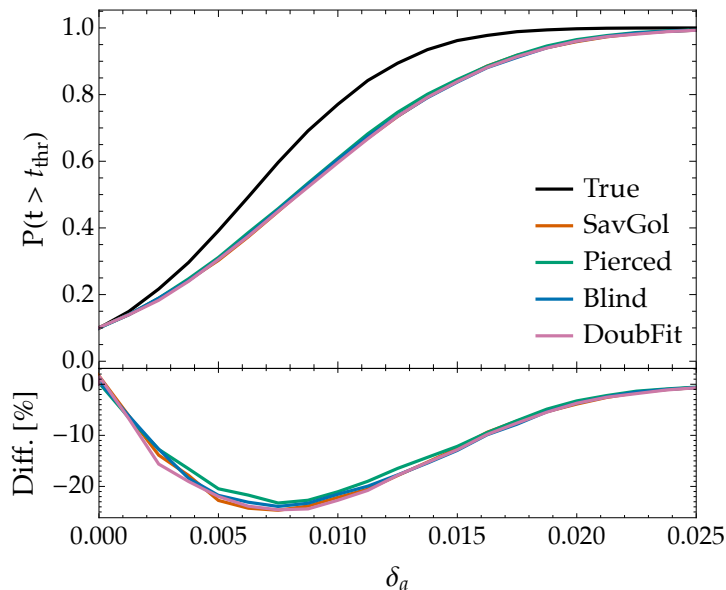


Figure 4: Same as Figure 3 with simulated data drawn from the baseline in Figure 5.

reconstructions and signal reduction. We have quantified the efficiency using two different approach: the definition of [53] and a Monte Carlo simulation.

Overall, the standard SG algorithm is the one most biased in the peak reconstruction. However, once the correlations among bins are taken into account, all the methods are characterized by the same efficiency in the reconstructed peak—within a few percent—and with the standard SG performing slightly better overall. For this reason, axion-search experiments such as ALPHA would not benefit from fancier extensions, more complex and more computationally intensive overall.

Acknowledgement

The Authors acknowledge support from the Knut and Alice Wallenberg Foundation and Olle Engkvists Foundation.

Appendix A SG filter

In this section, we report the calculation of the coefficients c_k appearing in (4), for the reader’s convenience. As the matter has extensively been dealt with in the literature, we will follow the reasoning as presented in Refs. [57–59].

Let us consider a vector of measured values \mathbf{y} , corresponding to some independent variable \mathbf{x} . In the case of the SG filtering, for instance, \mathbf{x} is

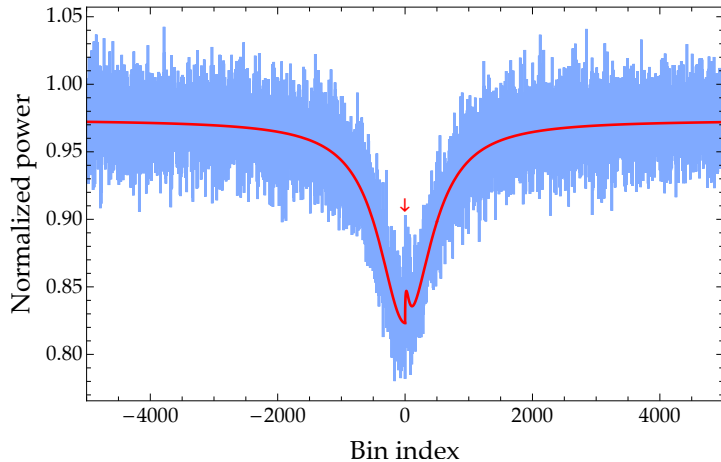


Figure 5: Simulated baseline with cryogenic quality factor $Q \sim 10^5$ and a resonance of 10 GHz.

built to encompass all the points around the filtered one. We are interested in fitting the measured values \mathbf{y} with a fitting function in polynomial form:

$$f(x) = \sum_{j=0}^n a_j x^j. \quad (13)$$

Note that the function is obtained as a fit around a specific bin x_i , and that the set of coefficient a_j depends on this particular choice through the N_p measured values that enter in the fit. However, carrying the bin index i would have made the notation unnecessarily heavy.

The coefficients a_j are chosen to minimize the mean-squared approximation error for the group of input samples:

$$\mathcal{E} = \sum_{\ell=0}^{N_p-1} ([\mathbf{f}]_{\ell} - [\mathbf{y}]_{\ell})^2, \quad (14)$$

where we have defined

$$[\mathbf{f}]_{\ell} = f_{\ell} = f(x_{\ell}). \quad (15)$$

We can simplify the problem if we assume to deal with a series of equally-spaced points, as it happens for the applications discussed in this paper. In such a case, the absolute scale of the independent variable x is not important, as everything can get shifted and rescaled. In other words, we can define the index k as the (discrete) distance from the filtered value (now, zero):

$$\mathcal{E}_i = \sum_{k=-N_l}^{N_r} \left(\sum_{j=0}^n b_j k^j - y_k \right)^2. \quad (16)$$

²We did not explicitly write y_{k+N_l} , as we thought that y_k was clearer in highlighting

Differentiating by the b_j and setting the corresponding derivative equal to zero yields the set of $n + 1$ equations in $n + 1$ unknowns:

$$\sum_{j=0}^n \sum_{k=-N_l}^{N_r} k^{j+\ell} b_j = \sum_{k=-N_l}^{N_r} k^\ell y_k \quad \text{for } \ell = 0, \dots, n. \quad (17)$$

As the filtered value corresponds to the fit function evaluated at $k = 0$, the problem reduces to the calculation of just one coefficient, $[\mathbf{b}]_0$.

A clever way to deal with this problem is to express Equation (17) in matrix form:

$$(\mathbf{V}^T \cdot \mathbf{V}) \cdot \mathbf{b} = \mathbf{V}^T \cdot \mathbf{y}, \quad (18)$$

$$\mathbf{b} = (\mathbf{V}^T \cdot \mathbf{V})^{-1} \cdot \mathbf{V}^T \cdot \mathbf{y} \equiv \mathbf{H} \cdot \mathbf{y}, \quad (19)$$

where \mathbf{V} is known as Vandermonde's matrix:

$$[\mathbf{V}]_{kj} = k^j, \quad (20)$$

with $[\mathbf{V}]_{00} = 1$. The index j goes from 0 to the polynomial degree n , while each column needs to include the N_p points k , from $-N_l$ to $+N_r$.

To get the coefficients c_k in (4) we are helped by the following relations:

$$[\mathbf{V}^T \cdot \mathbf{V}]_{Kj} = \sum_k [\mathbf{V}]_{ki} [\mathbf{V}]_{kj} = \sum_k k^{i+j}, \quad (21)$$

$$[\mathbf{V}^T \cdot \mathbf{y}]_{kj} = \sum_k V_{kj} y_k = \sum_k k^j y_k. \quad (22)$$

Now, recapping, for the SG filtering we are interested in the point:

$$f(0) = b_0 = \sum_{k=-N_l}^{N_r} c_k y_k, \quad (23)$$

and ultimately in the set \mathbf{c} of coefficients. Those are easily obtained if we notice that c_k is exactly the output b_0 when all the components of \mathbf{y} are null but the k -th one. Thus, we can simply substitute \mathbf{y} with the unit vector \mathbf{e}_k :

$$c_k = \left[(\mathbf{V}^T \cdot \mathbf{V})^{-1} \cdot (\mathbf{V}^T \cdot \mathbf{e}_k) \right]_0 = \sum_{j=0}^n \left[(\mathbf{V}^T \cdot \mathbf{V})^{-1} \right]_{0j} k^j. \quad (24)$$

From Equation (24), we see that just the first row of matrix $(\mathbf{V}^T \cdot \mathbf{V})^{-1}$ is needed. Therefore, efficient computations can be implemented for such a purpose—see e.g. Section 2.3 in [58, 59].

that the boundaries have been properly shifted.

References

- [1] Vera C. Rubin and W. Kent Ford Jr. “Rotation of the Andromeda Nebula from a Spectroscopic Survey of Emission Regions”. In: *Astrophys. J.* 159 (1970), pp. 379–403. DOI: 10.1086/150317.
- [2] Yoshiaki Sofue and Vera Rubin. “Rotation curves of spiral galaxies”. In: *Ann. Rev. Astron. Astrophys.* 39 (2001), pp. 137–174. DOI: 10.1146/annurev.astro.39.1.137. arXiv: astro-ph/0010594.
- [3] P. J. E. Peebles. “Large scale background temperature and mass fluctuations due to scale invariant primeval perturbations”. In: *Astrophys. J. Lett.* 263 (1982). Ed. by M. A. Srednicki, pp. L1–L5. DOI: 10.1086/183911.
- [4] Volker Springel et al. “Simulating the joint evolution of quasars, galaxies and their large-scale distribution”. In: *Nature* 435 (2005), pp. 629–636. DOI: 10.1038/nature03597. arXiv: astro-ph/0504097.
- [5] Douglas Clowe et al. “A direct empirical proof of the existence of dark matter”. In: *Astrophys. J. Lett.* 648 (2006), pp. L109–L113. DOI: 10.1086/508162. arXiv: astro-ph/0608407.
- [6] E. Komatsu et al. “Five-Year Wilkinson Microwave Anisotropy Probe (WMAP) Observations: Cosmological Interpretation”. In: *Astrophys. J. Suppl.* 180 (2009), pp. 330–376. DOI: 10.1088/0067-0049/180/2/330. arXiv: 0803.0547 [astro-ph].
- [7] P. A. R. Ade et al. “Planck 2015 results. XIII. Cosmological parameters”. In: *Astron. Astrophys.* 594 (2016), A13. DOI: 10.1051/0004-6361/201525830. arXiv: 1502.01589 [astro-ph.CO].
- [8] Gianfranco Bertone, Dan Hooper, and Joseph Silk. “Particle dark matter: Evidence, candidates and constraints”. In: *Phys. Rept.* 405 (2005), pp. 279–390. DOI: 10.1016/j.physrep.2004.08.031. arXiv: hep-ph/0404175.
- [9] Stefano Profumo. *An Introduction to Particle Dark Matter*. World Scientific, 2017. ISBN: 978-1-78634-000-9.
- [10] Gianfranco Bertone and Tim Tait M. P. “A new era in the search for dark matter”. In: *Nature* 562.7725 (2018), pp. 51–56. DOI: 10.1038/s41586-018-0542-z. arXiv: 1810.01668 [astro-ph.CO].
- [11] Daniel Green et al. *Snowmass Theory Frontier: Astrophysics and Cosmology*. Tech. rep. 57 pages. Snowmass, 2022. arXiv: 2209.06854. URL: <https://cds.cern.ch/record/2827615>.
- [12] J. H. Smith, E. M. Purcell, and N. F. Ramsey. “Experimental limit to the electric dipole moment of the neutron”. In: *Phys. Rev.* 108 (1957), pp. 120–122. DOI: 10.1103/PhysRev.108.120.

- [13] W. B. Dress et al. “Search for an Electric Dipole Moment of the Neutron”. In: *Phys. Rev. D* 15 (1977), p. 9. DOI: 10.1103/PhysRevD.15.9.
- [14] Gerard 't Hooft. “Symmetry Breaking Through Bell-Jackiw Anomalies”. In: *Phys. Rev. Lett.* 37 (1976). Ed. by Mikhail A. Shifman, pp. 8–11. DOI: 10.1103/PhysRevLett.37.8.
- [15] Gerard 't Hooft. “Computation of the Quantum Effects Due to a Four-Dimensional Pseudoparticle”. In: *Phys. Rev. D* 14 (1976). Ed. by Mikhail A. Shifman. [Erratum: *Phys.Rev.D* 18, 2199 (1978)], pp. 3432–3450. DOI: 10.1103/PhysRevD.14.3432.
- [16] R. D. Peccei and Helen R. Quinn. “CP Conservation in the Presence of Instantons”. In: *Phys. Rev. Lett.* 38 (1977), pp. 1440–1443. DOI: 10.1103/PhysRevLett.38.1440.
- [17] R. D. Peccei and Helen R. Quinn. “Constraints Imposed by CP Conservation in the Presence of Instantons”. In: *Phys. Rev. D* 16 (1977), pp. 1791–1797. DOI: 10.1103/PhysRevD.16.1791.
- [18] Steven Weinberg. “A New Light Boson?” In: *Phys. Rev. Lett.* 40 (1978), pp. 223–226. DOI: 10.1103/PhysRevLett.40.223.
- [19] Frank Wilczek. “Problem of Strong P and T Invariance in the Presence of Instantons”. In: *Phys. Rev. Lett.* 40 (1978), pp. 279–282. DOI: 10.1103/PhysRevLett.40.279.
- [20] J. Preskill, M. B. Wise, and F. Wilczek. “Cosmology of the Invisible Axion”. In: *Phys. Lett. B* 120 (1983). Ed. by M. A. Srednicki, pp. 127–132. DOI: 10.1016/0370-2693(83)90637-8.
- [21] L. F. Abbott and P. Sikivie. “A Cosmological Bound on the Invisible Axion”. In: *Phys. Lett. B* 120 (1983). Ed. by M. A. Srednicki, pp. 133–136. DOI: 10.1016/0370-2693(83)90638-X.
- [22] M. Dine and W. Fischler. “The Not So Harmless Axion”. In: *Phys. Lett. B* 120 (1983). Ed. by M. A. Srednicki, pp. 137–141. DOI: 10.1016/0370-2693(83)90639-1.
- [23] Igor G. Irastorza and Javier Redondo. “New experimental approaches in the search for axion-like particles”. In: *Prog. Part. Nucl. Phys.* 102 (2018), pp. 89–159. DOI: 10.1016/j.pnpnp.2018.05.003. arXiv: 1801.08127 [hep-ph].
- [24] Julien Billard et al. “Direct detection of dark matter—APPEC committee report*”. In: *Rept. Prog. Phys.* 85.5 (2022), p. 056201. DOI: 10.1088/1361-6633/ac5754. arXiv: 2104.07634 [hep-ex].
- [25] Igor Garcia Irastorza. “An introduction to axions and their detection”. In: *SciPost Phys. Lect. Notes* 45 (2022), p. 1. DOI: 10.21468/SciPostPhysLectNotes.45. arXiv: 2109.07376 [hep-ph].

- [26] Yannis K. Semertzidis and SungWoo Youn. “Axion dark matter: How to see it?” In: *Sci. Adv.* 8.8 (2022), abm9928. DOI: 10.1126/sciadv.abm9928. arXiv: 2104.14831 [hep-ph].
- [27] C.B. Adams et al. *Axion Dark Matter*. Tech. rep. restore and expand author list. Snowmass, 2022. arXiv: 2203.14923. URL: <https://cds.cern.ch/record/2855525>.
- [28] D.F.J. Kimball and K. van Bibber, eds. *The Search for Ultralight Bosonic Dark Matter*. Springer Cham, 2022. ISBN: 978-3-030-95851-0.
- [29] Jihn E. Kim. “Weak Interaction Singlet and Strong CP Invariance”. In: *Phys. Rev. Lett.* 43 (1979), p. 103. DOI: 10.1103/PhysRevLett.43.103.
- [30] Mikhail A. Shifman, A. I. Vainshtein, and Valentin I. Zakharov. “Can Confinement Ensure Natural CP Invariance of Strong Interactions?” In: *Nucl. Phys. B* 166 (1980), pp. 493–506. DOI: 10.1016/0550-3213(80)90209-6.
- [31] Michael Dine, Willy Fischler, and Mark Srednicki. “A Simple Solution to the Strong CP Problem with a Harmless Axion”. In: *Phys. Lett. B* 104 (1981), pp. 199–202. DOI: 10.1016/0370-2693(81)90590-6.
- [32] A. R. Zhitnitsky. “On Possible Suppression of the Axion Hadron Interactions. (In Russian)”. In: *Sov. J. Nucl. Phys.* 31 (1980), p. 260.
- [33] P. Sikivie. “Experimental Tests of the Invisible Axion”. In: *Phys. Rev. Lett.* 51 (1983). Ed. by M. A. Srednicki. [Erratum: *Phys.Rev.Lett.* 52, 695 (1984)], pp. 1415–1417. DOI: 10.1103/PhysRevLett.51.1415.
- [34] Pierre Sikivie. “Detection Rates for ‘Invisible’ Axion Searches”. In: *Phys. Rev. D* 32 (1985). [Erratum: *Phys.Rev.D* 36, 974 (1987)], p. 2988. DOI: 10.1103/PhysRevD.36.974.
- [35] N. Du et al. “A Search for Invisible Axion Dark Matter with the Axion Dark Matter Experiment”. In: *Phys. Rev. Lett.* 120.15 (2018), p. 151301. DOI: 10.1103/PhysRevLett.120.151301. arXiv: 1804.05750 [hep-ex].
- [36] T. Braine et al. “Extended Search for the Invisible Axion with the Axion Dark Matter Experiment”. In: *Phys. Rev. Lett.* 124.10 (2020), p. 101303. DOI: 10.1103/PhysRevLett.124.101303. arXiv: 1910.08638 [hep-ex].
- [37] C. Bartram et al. “Search for Invisible Axion Dark Matter in the 3.3–4.2 μeV Mass Range”. In: *Phys. Rev. Lett.* 127.26 (2021), p. 261803. DOI: 10.1103/PhysRevLett.127.261803. arXiv: 2110.06096 [hep-ex].
- [38] Andrew K. Yi et al. “Axion Dark Matter Search around 4.55 μeV with Dine-Fischler-Srednicki-Zhitnitskii Sensitivity”. In: *Phys. Rev. Lett.* 130.7 (2023), p. 071002. DOI: 10.1103/PhysRevLett.130.071002. arXiv: 2210.10961 [hep-ex].

- [39] Swadha Pandey, Evan D. Hall, and Matthew Evans. “First results from the Axion Dark-Matter Birefringent Cavity (ADBC) experiment”. In: (Apr. 2024). arXiv: 2404.12517 [hep-ex].
- [40] C. Bartram et al. “Axion dark matter experiment: Run 1B analysis details”. In: *Phys. Rev. D* 103.3 (2021), p. 032002. DOI: 10.1103/PhysRevD.103.032002. arXiv: 2010.06183 [astro-ph.CO].
- [41] Yuka Oshima et al. “First results of axion dark matter search with DANCE”. In: *Phys. Rev. D* 108.7 (2023), p. 072005. DOI: 10.1103/PhysRevD.108.072005. arXiv: 2303.03594 [hep-ex].
- [42] Thierry Grenet et al. “The Grenoble Axion Haloscope platform (GrA-Hal): development plan and first results”. In: (Oct. 2021). arXiv: 2110.14406 [hep-ex].
- [43] D. A. Palken et al. “Improved analysis framework for axion dark matter searches”. In: *Phys. Rev. D* 101.12 (2020), p. 123011. DOI: 10.1103/PhysRevD.101.123011. arXiv: 2003.08510 [astro-ph.IM].
- [44] Aaron Quiskamp et al. “Exclusion of Axionlike-Particle Cogenesis Dark Matter in a Mass Window above 100 μeV ”. In: *Phys. Rev. Lett.* 132.3 (2024), p. 031601. DOI: 10.1103/PhysRevLett.132.031601. arXiv: 2310.00904 [hep-ex].
- [45] R. Di Vora et al. “Search for galactic axions with a traveling wave parametric amplifier”. In: *Phys. Rev. D* 108.6 (2023), p. 062005. DOI: 10.1103/PhysRevD.108.062005. arXiv: 2304.07505 [hep-ex].
- [46] S. Ahyoune et al. “RADES axion search results with a High-Temperature Superconducting cavity in an 11.7 T magnet”. In: (Mar. 2024). arXiv: 2403.07790 [hep-ex].
- [47] Alexander V. Gramolin et al. “Search for axion-like dark matter with ferromagnets”. In: *Nature Phys.* 17.1 (2021), pp. 79–84. DOI: 10.1038/s41567-020-1006-6. arXiv: 2003.03348 [hep-ex].
- [48] Hsin Chang et al. “First Results from the Taiwan Axion Search Experiment with a Haloscope at 19.6 μeV ”. In: *Phys. Rev. Lett.* 129.11 (2022), p. 111802. DOI: 10.1103/PhysRevLett.129.111802. arXiv: 2205.05574 [hep-ex].
- [49] Catriona A. Thomson et al. “Searching for low-mass axions using resonant upconversion”. In: *Phys. Rev. D* 107.11 (2023), p. 112003. DOI: 10.1103/PhysRevD.107.112003. arXiv: 2301.06778 [hep-ex].
- [50] Joshua W. Foster, Nicholas L. Rodd, and Benjamin R. Safdi. “Revealing the Dark Matter Halo with Axion Direct Detection”. In: *Phys. Rev. D* 97.12 (2018), p. 123006. DOI: 10.1103/PhysRevD.97.123006. arXiv: 1711.10489 [astro-ph.CO].

- [51] A. Savitzky and M.J.E. Golay. “Smoothing and Differentiation of Data by Simplified Least Squares Procedures”. In: *Analytical Chemistry* 36.8 (July 1964), pp. 1627–1639. ISSN: 0003-2700. DOI: 10.1021/ac60214a047. URL: <https://doi.org/10.1021/ac60214a047>.
- [52] Michael Schmid, David Rath, and Ulrike Diebold. “Why and How Savitzky–Golay Filters Should Be Replaced”. In: *ACS Measurement Science Au* 2.2 (2022), pp. 185–196. DOI: 10.1021/acsmesuresciau.1c00054.
- [53] A. K. Yi et al. “Analytical estimation of the signal to noise ratio efficiency in axion dark matter searches using a Savitzky-Golay filter”. In: *JHEP* 11 (2023), p. 115. DOI: 10.1007/JHEP11(2023)115. arXiv: 2310.07967 [astro-ph.IM].
- [54] B. M. Brubaker et al. “HAYSTAC axion search analysis procedure”. In: *Phys. Rev. D* 96.12 (2017), p. 123008. DOI: 10.1103/PhysRevD.96.123008. arXiv: 1706.08388 [astro-ph.IM].
- [55] Benjamin M. Brubaker. “First results from the HAYSTAC axion search”. PhD thesis. Yale U., 2017. arXiv: 1801.00835 [astro-ph.CO].
- [56] Michael S. Turner. “Periodic signatures for the detection of cosmic axions”. In: *Phys. Rev. D* 42 (1990), pp. 3572–3575. DOI: 10.1103/PhysRevD.42.3572.
- [57] Ronald W. Schafer. “What Is a Savitzky-Golay Filter? [Lecture Notes]”. In: *IEEE Signal Processing Magazine* 28.4 (2011), pp. 111–117. DOI: 10.1109/MSP.2011.941097. URL: http://andrewd.ces.clemson.edu/courses/cpsc881/papers/Sch11_whatIsSG.pdf.
- [58] William H. Press et al. *Numerical Recipes: The Art of Scientific Computing*. Second edition. Cambridge, USA: Cambridge University Press, 1992. ISBN: 978-0521431088. URL: <https://numerical.recipes/book.html>.
- [59] William H. Press et al. *Numerical Recipes: The Art of Scientific Computing*. Third edition. Cambridge, USA: Cambridge University Press, 2011. ISBN: 978-0521880688. URL: <https://numerical.recipes/book.html>.
- [60] Andrea Gallo Rosso, Sara Algeri, and Jan Conrad. “Sequential hypothesis testing for axion haloscopes”. In: *Phys. Rev. D* 108.2 (2023), p. 023003. DOI: 10.1103/PhysRevD.108.023003. arXiv: 2210.16095 [physics.data-an].
- [61] Alexander J. Millar et al. “Searching for dark matter with plasma haloscopes”. In: *Phys. Rev. D* 107 (5 Mar. 2023), p. 055013. DOI: 10.1103/PhysRevD.107.055013. URL: <https://link.aps.org/doi/10.1103/PhysRevD.107.055013>.